ISSN 1063-7397, Russian Microelectronics, 2024, Vol. 53, No. 4, pp. 339–348. © Pleiades Publishing, Ltd., 2024.

Al Islands on Si(111): Growth Temperature, Morphology, and Strain

A. A. Lomov[a], *, D. M. Zakharov[a], M. A. Tarasov[b], A. M. Chekushkin[b], A. A. Tatarintsev[a], and A. L. Vasiliev[c]

[a] *Valiev Institute of Physics and Technology, Russian Academy of Sciences, Moscow, 117218 Russia*

[b] *Kotel'nikov Institute of Radio Engineering and Electronics, Russian Academy of Sciences, Moscow, 125009 Russia*

[c] *National Research Center "Kurchatov Institute," Moscow, 123182 Russia*

**e-mail: lomov@ftian.ru*

Received March 5, 2024; revised April 25, 2024; accepted April 25, 2024

Abstract—Comprehensive structural studies of thin island Al films with a thickness of 20–50 nm deposited by magnetron sputtering on Si(111) substrates in an argon plasma at a pressure of 6×10^{-3} mbar and a temperature ranging from 20 to 500°C are presented. The morphology and microstructure of the films are studied using XRD, SEM, EDS, and TEM methods. It is found that most of the islands are Al {001} and Al {111} crystallites with lateral sizes of 10–100 nm, differently conjugated with the Si(111) substrate. At room temperature of the substrate, only Al {001} crystallites are epitaxially formed on it. The epitaxial growth of Al {111} crystallites is predominant as the substrate temperature increases above 400°C. The influence of the temperature of the Si(111) substrate on the process of epitaxial growth of crystallites, the dynamics of their shape, and structural perfection is shown. It is found that crystallites epitaxially connected to the substrate experience deformation at $\varepsilon = 7 \times 10^{-3}$ and $\varepsilon = -2 \times 10^{-3}$ for Al {001} and Al {111}, respectively. It is shown that for thin island Al films on Si(111), the dependence of the number of crystallization centers and the particle growth rate on the supercooling temperature is consistent with the band model of crystallization. At the same time, a shift in the characteristic temperatures for the zone boundaries is observed due to the properties of the substrate. This must be taken into account when engineering the surface morphology and structural perfection of crystallites in Al island magnetron films.

Keywords: aluminum, silicon, magnetron sputtering, epitaxy, morphology, microstructure, X-ray diffraction, SEM and TEM microscopy

DOI: 10.1134/S1063739724600468

1. INTRODUCTION

Due to its physical properties, aluminum is used in various applications in optoelectronics, microelectronics [1–3], solar energy [4, 5], micro- and nanomechanics [6], and superconducting devices [7–9]. It is worth noting that not only the traditionally used nanosized aluminum films (reflective coatings, integrated circuits, contacts, valves) but also aluminum crystallites as seeds for the formation of polysilicon [10] and nanoparticles [11] are of interest. Model Al-Si structures are formed to study the fundamental properties at the superconductor-semiconductor interface [12, 13]. Such diverse applications of aluminum require the development of old growth methods and the creation of new techniques for the formation of both single-crystalline and island films [10, 11]. Despite the existing growth models [14, 15], the use of various thermodynamic conditions during film growth, as well as a large number of parameters, does not allow us to unambiguously predict their properties in advance. The mechanical, electrical, and optical properties of aluminum films are determined by their composition, surface morphology, and microstructure. Among various methods for producing thin films on various substrates, magnetron sputtering occupies a special place due to the convenience of forming multilayer systems and device structures. It was shown in [16] that the magnetron sputtering method can control the properties of aluminum films on the surface of Si(111) substrates, forming on their surface at a temperature of 400°C island homobuffer Al layers. It is well known [17] that at these temperatures the solubility limit and diffusion of Si in Al, compared to aluminum, sharply increases. This leads to the loss of a sharp boundary between the film and the substrate due to the formation of voids and precipitates in the film (Kirkendall effect [18]). The presence of such a layer will affect the fundamental properties of nanosized films and structures based on them. This is especially important for superconducting films. Such a transition layer, which is inhomogeneous in density, for example, will change the charge density at the interface with the substrate and create additional scattering of conduction electrons. The question of the sharpness of the boundary between the silicon substrate and

aluminum crystallites is related to the use of such structures in various applications: contacts in VLSI circuits, superconducting high-quality resonators, microwave oscillators and amplifiers, bolometers, and gates in quantum devices. Naturally, blurring the boundary between the silicon substrate and the aluminum film and the formation of structural defects in it can reduce the efficiency of the devices being created.

The ability to epitaxially bond silicon and aluminum to produce a sharp interface and an atomically smooth film surface continues to be a key issue in the development of magnetron sputtering technology. First of all, the main growth conditions include the substrate and film materials used, the phase state of the substrate and its crystallographic orientation, the substrate temperature, the cleanliness and smoothness of the substrate surface, the plasma operating pressure, the residual gas pressure in the chamber, the energy of atoms, and the rate of their deposition. The microstructure of the films being formed will be greatly influenced by the deformation fields created by the surface atoms of the substrate. The presence of such an orienting influence of the substrate on adatoms leads to the phenomenon of epitaxy [19].

Usually, during magnetron sputtering, island growth of a polycrystalline aluminum film occurs according to the Volmer-Weber method [20]. To achieve the main goal of obtaining an atomically smooth aluminum film, it is desirable to form a well-textured quasi-epitaxial film consisting of large crystallites. The crystallization process, as pointed out by D.K. Chernov and experimentally shown G. Tamman [21], can be quantitatively described in terms of the crystallite size $d \propto V_g/N_n$, where their growth rate $V_g(\Delta T)$ and nucleation rate $N_n(\Delta T)$ is determined by the amount of subcooling of the substrate relative to the melting temperature $\Delta T = T_{melt} - T_r$. This position was confirmed in the works of Movchan and Demchishin [22], who proposed the zone model of crystallization (ZMC) based on the analysis of the experimental data. In the ZMC model, depending on the ratio of the growth and melting temperatures T_s/T_{melt}, zones and their boundaries are introduced [15, 22–24]. According to the ZMC, the microstructure of island films is determined by their belonging to the corresponding zone. Developing the ZMC, Thornton [25] added a fourth transition zone T. The zone boundary temperatures are determined based on an analysis of the actual structure of continuous films and depend on the method of their formation [23]. In the ZMC model, films with a pronounced texture are formed in the second zone, and large crystallites with different faceting in the third zone. The temperature value for the zone boundaries is conditional. For example, Al films grown under the same conditions on Si(111) substrates with different surface morphologies have different textures and mechanical properties [16] and, in principle, should belong to different zones. Despite the existing general patterns in the formation of crystallites, the process of their growth, taking into account the additionally involved physical phenomena, cannot be modeled during the formation of continuous films. Often in the literature, the results of studying films are presented with a statement of the growth conditions, but without an analysis of their influence on the process itself.

During the magnetron sputtering of metals and, in particular, aluminum, a polycrystalline film is formed on the surface of the substrate [26]. For metals with an FCC lattice, in most cases a textured film is formed, whose crystallites are predominantly oriented along the normal to the substrate surface with the [111] axes [23–26]. Single-crystal Al(111) films on an Si(111) substrate were grown by the authors of [19] by the MBE method despite the 25.3% difference in the crystal lattice parameters of Al ($a = 0.405$ nm) and Si ($a = 0.543$ nm) at room temperature. The appearance of such a possibility of accommodation of two structures at the (111) boundary is related to the coincidence of every third silicon atom with the fourth aluminum atom. In this case, the mismatch of the lattices is only 0.6%. The growth of epitaxial Al(001) crystallites on the Si(111) substrate is also probable and was observed in [27, 28]. It should be noted that for elements with a cubic structure, faceting of crystallites by the {001} planes at the initial stages of growth is preferable [29]. The formation of structurally perfect crystallites is determined by the processes of the surface and volume diffusion of adatoms. A large diffusion length promotes stepwise growth of crystalline planes, filling potential vacancy voids as they form from the residual gases present in a vacuum system. Due to volumetric diffusion, adatoms reach their equilibrium position in the crystallite lattice. The growth and orientation of crystallites is determined by a complex of processes accompanying the surface diffusion of the deposited adatoms. Note that the nucleation and growth of a crystallite is accompanied by the formation of various structural defects both inside it and at the interface with the substrate. First of all, for selected materials, the diffusion of adatoms depends on their energy (growth method) and activation energy of the substrate surface (temperature, deformation of the surface layer) [14, 15, 23, 29].

A deeper understanding of the effect of temperature on the morphology and microstructure of island films can be obtained by studying free-standing crystallites at the initial stage of their growth. This paper studies the influence of the Si(111) substrate temperature on the microstructure of crystallites and interphase boundaries of thin Al island films obtained by magnetron sputtering.

2. EXPERIMENTAL

Samples of thin Al island films on standard Si(111) substrates with a thickness of 350 μm were obtained

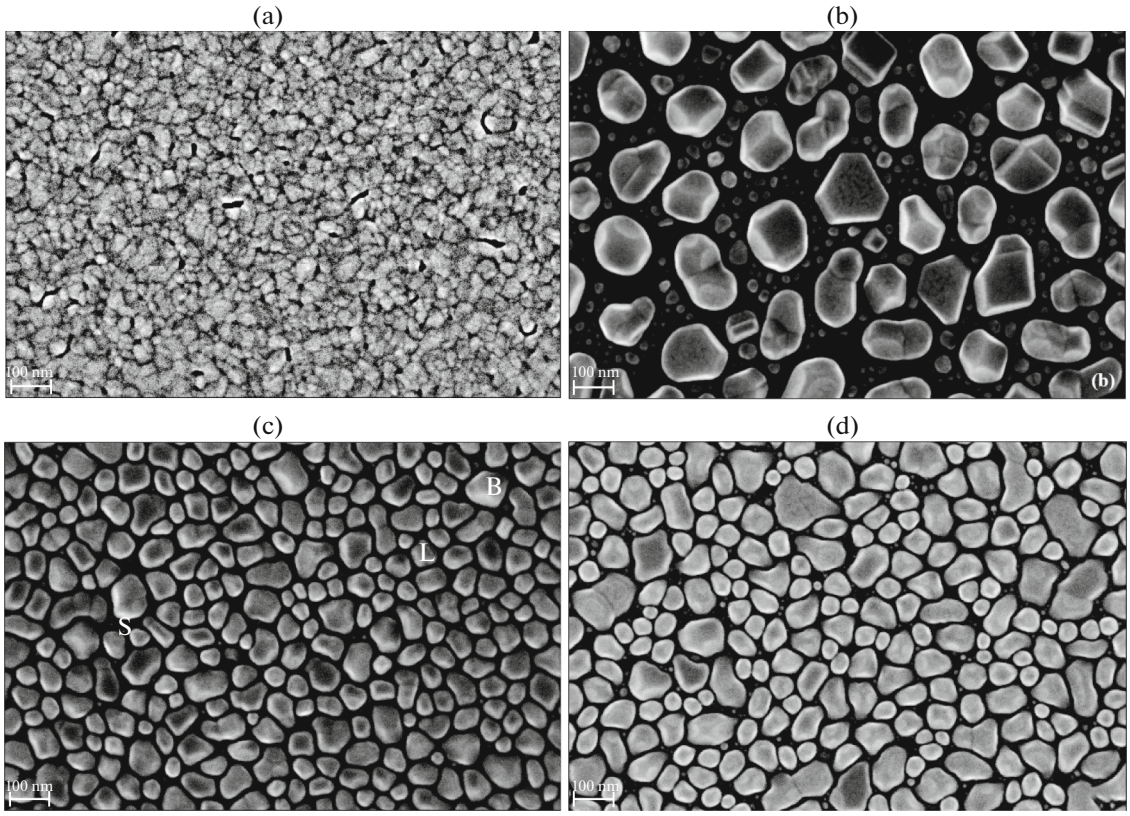

Fig. 1. SEM images of the surface of magnetron sputtered Al films with an average thickness of 20–50 nm, formed in a steady state on an Si(111) substrate at a temperature of 20 (a), 200 (b), 400 (c), and 500°C (d). The letters B, L, and S (c) indicate crystallites with characteristic sizes.

using a magnetron sputtering installation (Kurt J. Lesker Company Ltd., Germany) in the discharge mode at a constant current and power of 500 W. The deviation of the (111) crystal planes from the substrate surface was 3.5 degrees. An aluminum target with a purity of 99.995% was used. Before film deposition, Si(111) substrates were cleaned in an ultrasonic bath in acetone. The remaining contaminants were washed off with distilled water. Then the substrates were sent to the deposition chamber, where an aluminum film was deposited on them. The films were formed at different substrate temperatures: 20, 200, 400, and 500°C. The rate and time of deposition of aluminum particles onto the substrate were 0.2 nm/s and 100 s, respectively. The residual gas pressure in the growth chamber depended on the growth temperature and was $(2–4.5) \times 10^{-7}$ mbar. The Al film deposition process took place in an argon atmosphere at a pressure of 6×10^{-3} mbar.

The morphology, microstructure, and composition of Al films were studied by electron microscopy in the SEM, EDS, TEM, STEM, RHEED, and X-ray diffractometry XRD modes. XRD diffractometry curves were obtained on a SmartLab X-ray diffractometer (9 kW, CBO optics, CuK_α radiation) in the geometry of a parallel beam. The diffraction patterns in the $\omega/2\theta$ scanning mode were recorded with a Soller slit of 0.114° installed in front of the detector window.

Electron microscopic images of the film crystallites were obtained at an accelerating voltage of 200 kV on an Osiris transmission/scanning electron microscope (ThermoFisher Scientific, United States) equipped with a high-angle dark-field detector (Fischione, United States) and a SuperX energy-dispersive X-ray microanalysis system (Bruker, United States). Images of the film surface and sample chips were obtained using a Carl Zeiss Ultra 55 scanning microscope equipped with an Oxford Instrument INCA X-act (EDS) energy dispersive spectrometer.

3. RESULTS AND DISCUSSION

3.1 SEM Microscopy

Images of the surface of the obtained Al/Si(111) magnetron films depending on the substrate temperature during sputtering are shown in Figs. 1a–1d. The surface morphology of the samples shows a strong dependence on the temperature of the shape, size, and relative position of the islands in the film.

When discussing the electron microscopy data, we will assume that the amount of aluminum sputtered

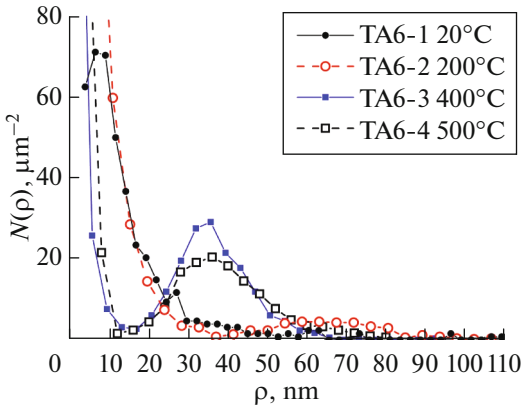

Fig. 2. Distribution of the number N(ρ) of Al islands on the Si(111) substrate depending on the radius ρ of the circle with an area equal to the area of the island in the SEM image.

onto the substrate is constant and there is no desorption. Figure 1a shows that the TA6-1 film is 22 nm thick (Table 1), grown at room temperature, and consists of islands tightly adjacent to each other. They contain rare voids in the form of holes with an average diameter of 20 nm or bands up to 70 nm in length. The appearance of the film shows that under the selected sputtering conditions and subcooling temperature $\Delta T = 640$ K ($T_s/T_{melt} = 0.3$), the atoms are low-mobile, evenly distributed over the surface of the sample, and form a continuous film. This conclusion is in accordance with the zone model of crystallization at significant supercooling. A large number of crystallization centers and their uniform growth form islands with an average size of 20 nm and various shapes. The shape of the islands on the surface of the film is drop-shaped. During the growth of the TA6-2 film, the supercooling temperature was reduced to $\Delta T = 440$ K, which corresponds to a value of $T_s/T_{melt} = 0.5$. An increase in the surface diffusion coefficient with temperature should lead to an increase in the growth rate of the islands in the film, which is observed in Fig. 1b. The film thickness increased to $h_z = 46$ nm. It is clearly seen that despite the steady flow of aluminum ions onto the substrate, the number of crystallization centers has decreased while the size of the islands has simultaneously increased. In addition to large islands, smaller islands are observed. The size distribution of the islands corresponds to a bimodal distribution. Around these main crystallites, there is an empty diffusion field formed by the escape of aluminum adatoms from it to the growing faces. Islands with faces symmetrical relative to the normal to the surface are individual crystallites. Similar results for the growth of large Al particles at $T = 500$ K were observed in [30]. The pronounced edges of these islands indicate a fairly high concentration of atoms during their growth. In contrast, near large circular islands, apparently, the concentration of aluminum atoms was insufficient for the growth of faces or desorption of atoms from their surface took place. The larger lateral L_x size of crystallites with voids between them and increased thickness h_z of the film indicates the formation of a thin film with a nonuniform density at the interface with the substrate. This circumstance should significantly affect its physical properties.

Aluminum films of samples TA6-3 (Fig. 1c) and TA6-4 (Fig. 1d) were sputtered at a supercooling temperature of 260°C ($T_s/T_{melt} = 0.7$) and 160°C ($T_s/T_{melt} = 0.8$), respectively. According to the zone growth model [22–25], the islands in these films should be crystallites with differently oriented and uniformly developed faces. The thick films grown under these conditions should be less textured. The SEM images of the surface of these films show that the size distribution of their islands, with a few exceptions, differs little. The thicknesses of the TA6-3 and TA6-4 films are 25 and 38 nm, respectively. In these films, small (S), main (L), and large (B) islands can be distinguished (Fig. 1c). The average size L_x of the islands is 70 nm. A detailed analysis of the images in Figs. 1c and 1d shows that the film of sample TA6-4, sputtered at a lower supercooling temperature, has a lower density. It repeats the effect of the formation of a diffusion field around large islands (Fig. 1b). An additional argument for the lower film density relative to the TA6-3 sample can be the increase in its thickness by 1.5 times while maintaining the sputtering time.

Figure 2 shows the lateral distributions $N(\rho)$ of the islands by radius ρ of equivalent areas in the form of a circle. The distribution curves were obtained using the Gwyddion v2.60 program (http://gwyddion.net/),

Table 1. Average sizes of crystallites (D), islands (S_x, L_x), and thickness h_z of Al/Si(111) film depending on the sputtering temperature

Samples, growth temperature	Crystallite size D, nm (XRD)			Island size, nm (SEM)		
	(111)	(200)	(220)	$\langle S_x \rangle$ (small islands)	$\langle L_x \rangle$ (main islands)	$\langle h_z \rangle$ (film thickness)
TA6-1, 20°C	8	23	20	15 ± 5	20 ± 10	22 ± 2
TA6-2, 200°C	14	25	–	30 ± 10	130 ± 30	46 ± 4
TA6-3, 400°C	18	21	11	15 ± 5	70 ± 20	25 ± 4
TA6-4, 500°C	19	16	7	13 ± 5	70 ± 25	38 ± 4

which allows for the statistical processing of images of both individual islands and islands joined together. For individual Al islands in films of samples TA6-2, 3, and 4, the distribution $N(\rho)$ was formed based on averaging a family of distribution curves over the threshold value with a step of 4 nm. Distribution $N(\rho)$ for the film of sample TA6-1 was obtained by increasing the image contrast in the segmentation mode with a step of 2.5 nm.

3.2. X-ray Diffractometry

The microstructure of the films of the studied samples was studied on the basis of X-ray diffraction patterns presented in Figs. 3a–3d. Each figure shows two diffraction patterns recorded without taking into account (1) and taking into account the precise (2) adjustment of the substrate to the diffraction reflection of Si(111). Let us recall that Bragg peaks or *hkl* reflections in diffraction patterns appear only when the normal to the crystalline plane of the island or substrate matrix lies in the diffraction plane. The diffraction plane is formed by the vectors of the incident and reflected X-ray waves. With the standard ω/2θ scheme while recording a diffraction pattern, the Bragg reflection from a scattering particle, whose crystal planes are parallel to the surface of the sample, enters the detector. When studying powders or ordinary polycrystalline films, crystallites that satisfy this requirement are always found. If, by tilting the sample, the normal to the selected crystalline plane of the particle is removed from the diffraction plane, the detector will not register the diffraction signal. The same reasoning applies to the Bragg reflection from the (111) crystal planes deviated from the surface of the Si substrate. The position of the sample at which the maximum reflection of Si(111) from the substrate is observed corresponds to its fine tuning (2) or alignment. Therefore, in the diffraction patterns, depending on the degree of alignment of the substrate or film islands, the corresponding Bragg reflections may appear or disappear.

Figures 3a–3d show the diffraction patterns from the studied samples in the angular range of $2\theta = 35°–70°$. Bragg 111 and 333 reflections from the Si(111) substrate at angles of $2\theta = 28.44°$ and 94.94° are outside the selected angular scanning region and are not observed in the diffraction patterns. The diffraction patterns show weak peaks near angles $2\theta = 38.48°$, 44.73°, and 65.11°, corresponding to reflections 111, 200, and 220 for the FCC Al lattice. It can be seen that the number of Bragg peaks, as well as their intensities, angular positions, and half-widths depend on both the film growth temperature and the alignment of the Si(111) substrate (curves (*2*) in Figs. 3a–3d). The relationship between the appearance of peaks or an increase in their intensity when the substrate is aligned indicates the presence of epitaxial (111) and (001) crystallites. Note that some of the crystallites are located on the surface of the substrate without epitaxy—they are not oriented by the crystal planes of the substrate (for example, the parameters of the 111 reflection peak in Fig. 3a do not change). It is clearly seen from the diffraction patterns (Fig. 3b) that the microstructure of the Al film formed at a temperature of 200°C is fundamentally different from the others; when the substrate is aligned, the 002 reflection peak sharply decreases. This dependence of the type of diffraction patterns

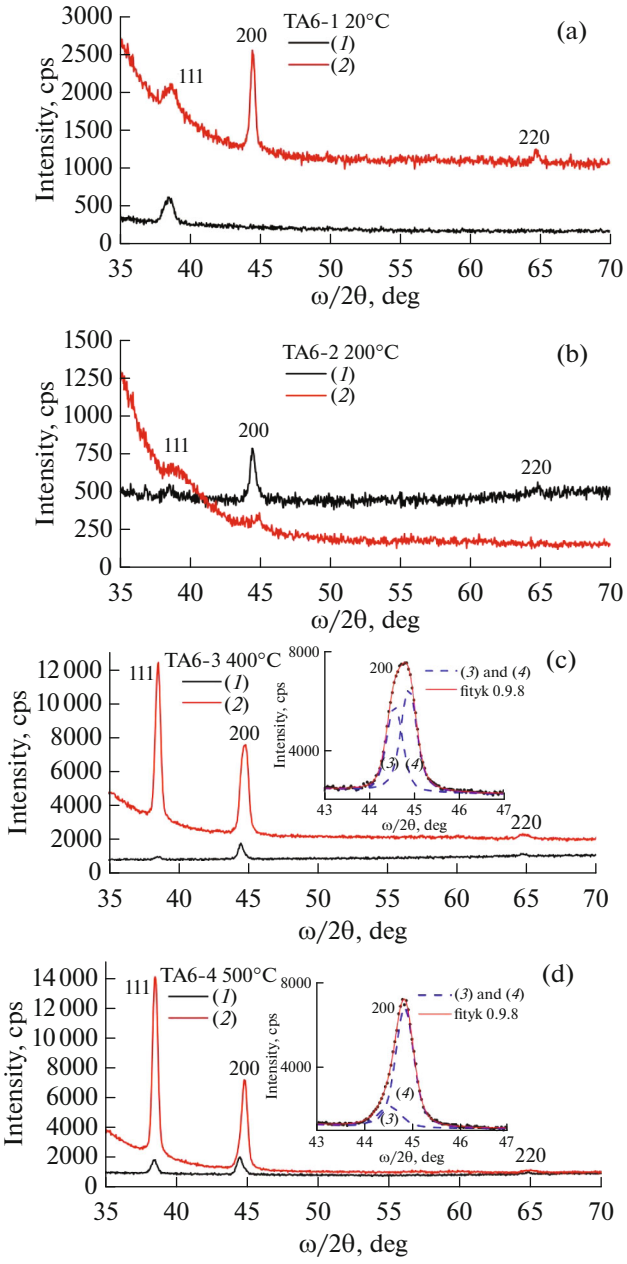

Fig. 3. Diffraction patterns from thin island films of Al/Si(111) sputtered at different substrate temperatures: 20°C (a), 200°C (b), 400°C (c), and 500°C (d). (*1*) Without fine tuning of the Si(111) substrate, (*2*) with fine tuning of the Si(111) substrate. The insets show a simulation of the 002 reflection peak using two Voigt curves at $2\theta = 44.55°$(*3*) and 44.85° (*4*). CuK_α radiation.

Table 2. Double Bragg angle values of $2\theta_{hkl}$ of reflections from crystallites of thin island films of Al/Si(111) depending on the alignment of the substrate during a diffraction experiment

Samples, growth temperature	XRD		XRD with substrate alignment		XRD (PDXL no. 03-065-2869)	
	$2\theta_{111}$, deg	$2\theta_{200}$, deg	$2\theta_{111}$, deg	$2\theta_{200}$, deg	$2\theta_{111}$, deg	$2\theta_{200}$, deg
TA6-1, 20°C	38.46(5)	–	38.66	44.47	38.47	44.72
TA6-2, 200°C	38.52(5)	44.45/44.80	38.86(5)	44.84	–	–
TA6-3, 400°C	38.52(5)	44.49	38.55	44.57/44.89	–	–
TA6-4, 500°C	38.52(5)	44.53	38.54	44.53/44.85	–	–

(Fig. 3b) shows that large crystallites with Al(001) faces are preferably located parallel to the substrate surface rather than to the Si(111) crystalline planes. The rotation of Al(001) crystallites from the planes of the Si(111) substrate with a misorientation of 3.5° due to dislocations at the boundary was observed for films 200 nm thick [31]. Note that for this sample, the DC signal intensity for the sample position without alignment is more than 2 times the background level. All this indicates the absence of epitaxy of (002) crystallites and the presence of a large number of structural defects (dislocations) at the film–substrate interface.

When the substrate temperature increases to 400°C, in the diffraction patterns (Fig. 3c), there is a sharp increase and narrowing of the 111 reflection peak, and the 002 reflection peak bifurcates. The latter observation is illustrated in the inset to Fig. 3c by modeling the 002 diffraction reflection peak with two Voigt profiles at $2\theta = 44.57°$(*3*) and 44.89° (*4*). The formation of an island film on a substrate at a temperature of 500°C only leads to quantitative changes in the shape and intensity of the peaks in the diffraction pattern (Fig. 3d). The relationship between the width of the diffraction peak and the crystallite size D (Table 1) without taking the microstresses into account is expressed through the Scherrer formula [20, 23]:

$$D = \frac{K\lambda}{W(2\theta)\cos(\theta_B)}, \quad (1)$$

where $W(2\theta)$ is the peak width at half its height, θ_B is the Bragg angle, λ is the radiation wavelength, and $K \sim 0.94$. The angular position values $2\theta_{hkl}$ of the peaks in the diffraction patterns (Fig. 3) are presented in Table 2. Their values make it possible to estimate the deformation $\varepsilon = \Delta d/d$ of the aluminum crystallites due to the contact with the substrate and possible structural defects in the bulk of the crystallite and at its boundary. The size of the deformation ε of the crystallites was estimated using the formula

$$\Delta d/d = -\cot\theta(\theta_{hkl} - \theta_0), \quad (2)$$

where θ_0 is the Bragg angle for the corresponding reflection of aluminum from the lattice constant a = 0.40497 nm (PDXL no. 03-065-2869).

Analysis of the angular data in Table 2 shows that the position of the diffraction peaks depends on the orientation of the crystallites and the temperature of the substrate during the formation of the island film. The most noticeable shifts in the Bragg angles for the 002 reflection relative to the table values are observed for the epitaxially grown crystallites in the temperature range 200–500°C. These crystallites are stretched normal to the surface by $\varepsilon \sim 3.2 \times 10^{-3}$. Some of the crystallites, which apparently experienced stress relaxation and lost their elastic connection with the substrate, have a reduced interplanar distance and compressive strain $\varepsilon \sim -3.2 \times 10^{-3}$. This effect can be related to both the presence of vacancies in the bulk of an aluminum crystallite [32] and with the manifestation of the Kirkendall effect—the formation of voids in the film at the boundary with the silicon substrate [18, 23]. Crystallites that have no connection with the substrate and are randomly located relative to the S(111) crystalline planes (Fig. 3a) have a Bragg angle equal to the tabulated value for powders. Apparently, these crystallites are poorly bonded to the silicon lattice and can increase the electrical resistance at the interface. The epitaxy of crystallites 111 appears when forming an Al film on a heated substrate at 400°C (Figs. 3c, 3d). An increase in the Bragg angle for the 111 reflection (Table 2) corresponds to compression of the crystallite lattice normal to the surface and the magnitude of the deformation of $\varepsilon \sim -1.9 \times 10^{-3}$. A more detailed analysis of the structural defects in island films of aluminum on silicon and their influence on the properties of the formed structures requires additional research.

Analysis of the X-ray diffraction patterns and Bragg angles for the 111 and 002 reflections from Al crystallites (Table 2) shows that at the initial stage of magnetron sputtering, crystallites with (111) and (001) orientations are formed on the Si(111) substrate. The (001) crystallites are the first ones to be epitaxially bonded to the substrate. As the substrate temperature increases, epitaxial crystallites (111) appear. Their number begins to predominate due to the smaller (4 : 3) mismatch between the parameters of the crystal lattices of silicon and aluminum.

3.3. TEM, STEM, and RHEED Microscopy

Two types of samples were prepared for research: in plane and cross sections. A schematic diagram of a TEM experiment for an in plane sample is shown in Fig. 4a. The sample was prepared by the classical method of ion etching in a Gatan PIPS installation (Gatan, United States). To conduct research, a ~1 mm section was separated from a sample of a silicon substrate with an aluminum film. Then the substrate part of the sample was thinned from the back side by mechanical grinding to a thickness of ~100 μm. A copper ring with a diameter of 3 mm and a thickness of 100 μm was glued to the back side of the sample prepared in this way with epoxy resin. The process of ion etching of the sample was carried out by beams of Ar^+ ions with an accelerating voltage of 5 kV at angles of 10–150 degrees from the substrate. After the through hole was formed in the aluminum film, cleaning was carried out at an accelerating voltage of 1.5 kV. Transverse sections were prepared using the standard focused ion beam method using a Versa dual beam electron ion microscope (ThermoFisher Scientific, United States). Before starting the procedure, a layer of Pt was sputtered onto the surface of the sample.

A bright-field TEM in plane image of an Al film of sample TA6-3 is shown in Fig. 4b. It shows individual particle islands with a size of 50–70 nm and fusions of two islands of length ~100 nm. Intergrowths are formed due to the effect of surface recrystallization of differently oriented islands. The image confirms the island mechanism of Al film formation. The islands are located chaotically. The lateral sides of the islands are either round or consist of straight sections. Despite the irregular arrangement of the islands, it is clearly visible that their sides with straight sections are approximately parallel along certain directions with an angle of 120 degrees between them.

Figure 4c shows the electron diffraction pattern obtained from sample TA6-3. Reflections from the silicon substrate with the [111] zone axis and a number of weak rings from the islands are clearly visible. The rings for reflections 111 and 220 are indicated by the arrows on the diffraction reflection intensity distribution curve. Analysis of the electron diffraction pattern shows a discrepancy between the ring intensities (see the radially averaged 2D pattern in Fig. 4c) and the structure factor of the FCC-Al peaks. The intensity of peak 111 is lower than the intensities of peaks 200 and 220. This effect confirms the presence of a preferred orientation of crystallites—the azimuthal texture of the aluminum film. The absence of ellipsoidal shape distortions and variations in the scattering intensity along the rings proves the absence of ordering for an array of crystallites in the azimuthal plane and is consistent with the model [33]. The data in Fig. 4 show that an aluminum film grown at a temperature of 400°C is mosaic despite the presence of individually oriented islands in it.

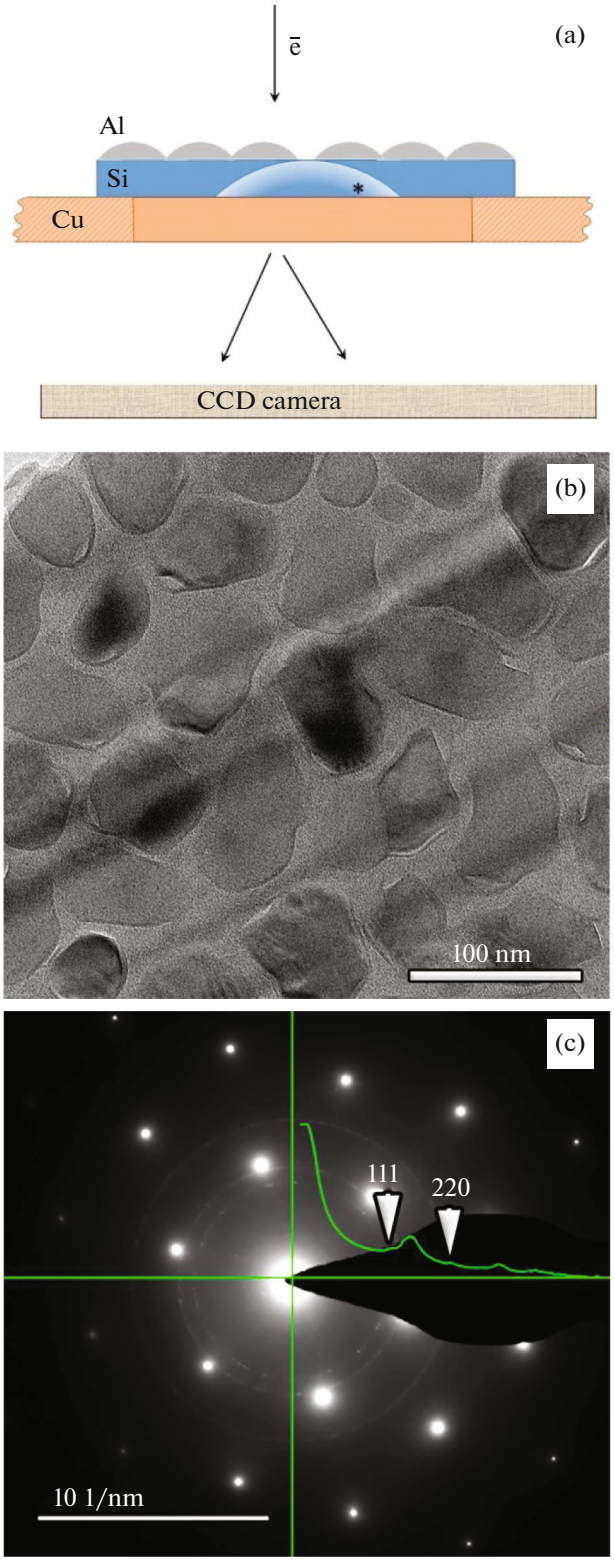

Fig. 4. Scheme of the TEM experiment (a), bright-field TEM image in plane of the Al film (sample TA6-3) (b) and its electron diffraction pattern (c).

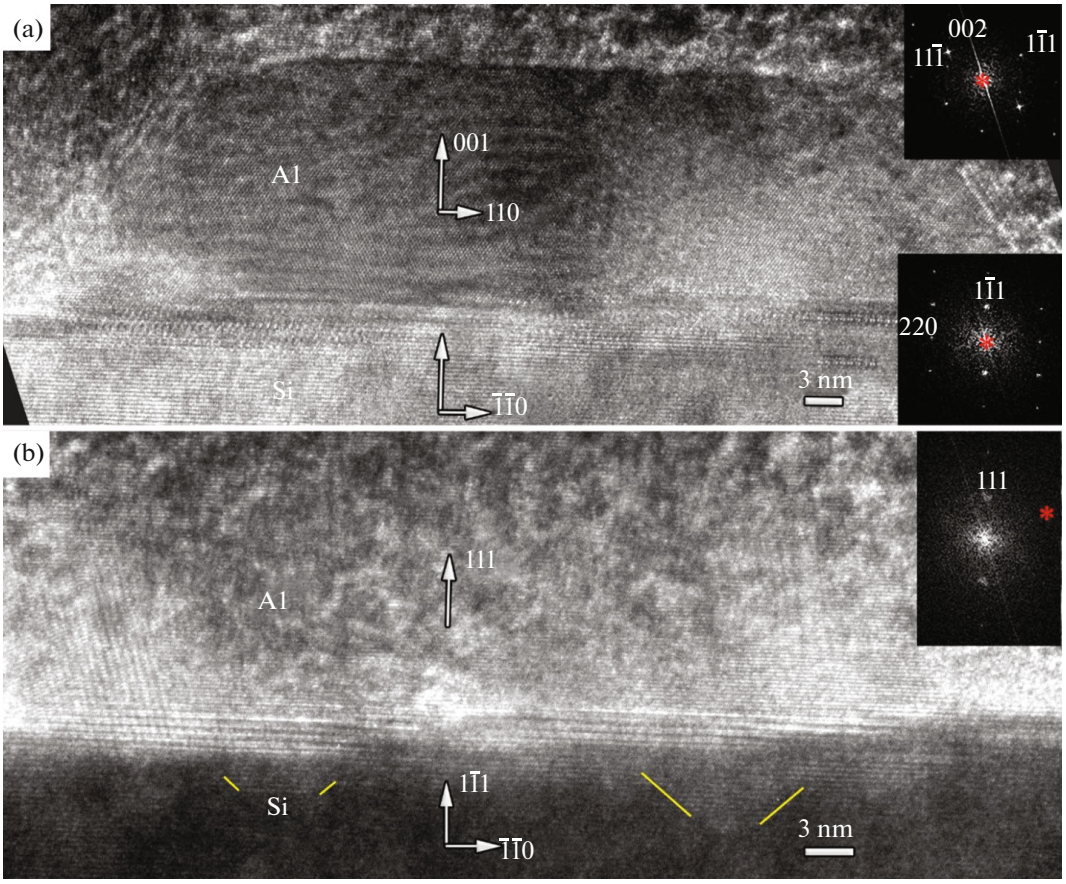

Fig. 5. (a) High-resolution bright-field STEM images of cross sections of a 23-nm-thick Al island film on an Si(111) substrate (growth at 400°C): (a) Al island with [001] orientation along the [111] normal to the substrate surface; (b) Al island with [111] orientation along the [111] normal to the substrate surface. The insets on the right show the 2D Fourier spectra from the corresponding crystal lattices of the Al islands (top) and the substrate (bottom).

To test the effect of the substrate on the formation of Al islands, a cross section of sample TA6-3 was prepared and examined (Fig. 5). The STEM image (Fig. 5a) shows an island-crystallite with a thickness of ~22 nm with a side cut close to the aluminum {111} planes. The orientation relations for this island are as follows: [001]Al//[1$\bar{1}$1]Si, [110]Al//[$\bar{1}\bar{1}$0]Si.

An example of a STEM image of a neighboring island is shown in Fig. 5b. Only one orientation relation is reliably determined: [111]Al//[1$\bar{1}$1]Si. The second orientation relation for this orientation is not determined due to the significant deviation of the Al crystal lattice from the low-index zone axis.

The TEM studies show that most of the large islands in the aluminum film of sample TA6-3 are crystallites with (001) and (111) faces parallel to the surface of the Si(111) substrate. Intermediate layers of other phases (for example, natural oxides, etc.) are not observed at the boundary between the crystallites and silicon planes. These results confirm the epitaxial intergrowth of aluminum crystallites with silicon at temperatures below the eutectic point equal to 577°C. It is known [23] that thermal annealing of Al/Si structures in the temperature range 400–500°C creates good ohmic contact between the metal and the semiconductor through the microalloy. During melting, the remnants of the oxide layer dissolve. This effect was observed previously [27] for Al(111)/Si(001) after thermal annealing at a temperature of 450°C. The disadvantage of thermal annealing is liquid-phase epitaxy in silicon, which leads to the formation of Si(Al) spikes in the substrate matrix at the film interface [23]. The presence of moiré at the interface and the contrast features in Fig. 5b indicate the formation of an Si(Al) solid solution in the form of spike-pyramids (marked by oblique markers) 3–5 nm in size in the substrate matrix.

Energy dispersive X-ray microanalysis (EDS) was used to obtain the data on the composition of the studied samples, obtained at an electron beam energy of 5 keV. The data from the quantitative EDS analysis of the samples, averaged over five points on the film surface, are presented Table 3.

From the data presented, it is clear that the composition of the near-surface layers of the samples, which

Table 3. Composition of the studied Al/Si(111) samples according to X-ray microanalysis (EDS)

Sample	at % C	at % O	at % Al	at % Si
TA6-1	7.55	2.64	5.66	84.15
TA6-2	7.62	2.53	6.37	83.48
TA6-3	7.91	3.12	6.57	82.39
TA6-4	7.88	3.14	6.82	82.16

includes thin island films of Al on an Si(111) substrate, is the same within the measurement error. The increased oxygen composition by 0.6% in films of samples TA6-3 and TA6-4 grown at 400 and 500°C is related to the increased residual gas pressure in the sputtering chamber due to temperature.

CONCLUSIONS

This paper presents the results of comprehensive studies of the influence of the temperature of a Si(111) silicon substrate on the surface morphology and microstructure of thin aluminum island films with a thickness of 20–50 nm grown by magnetron sputtering at a pressure of 6×10^{-3} mbar in argon. The experiments were performed using X-ray diffractometry, as well as scanning and transmission electron microscopy. The sizes of aluminum crystallites, their structural perfection, and the sequence of epitaxy and stress relaxation depending on the substrate temperature are determined. It has been established that at room temperature of the Si(111) substrate, the epitaxial growth of aluminum islands begins with Al {001} crystallites. The epitaxial growth of Al {111} crystallites begins to be predominant with the substrate temperature increasing above 400°C due to the changes in thermodynamic conditions. It has been confirmed that at a temperature of 400–500°C, the formation of Al crystallites leads to the blurring of the natural oxide layer at the interface with the Si(111) substrate and the appearance of a ~5-nm dendritic transition layer of the solid solution.

It has been established that in Al island films on Si(111), the dependence of the number of crystallization centers and the particle growth rate on the supercooling temperature is qualitatively consistent with the model of crystallization of metal particles from a melt [21]. The zone model of crystallization of islands is greatly influenced by the temperature-dependent parameter of the crystal lattice of the substrate. At a substrate temperature of 200°C ($T_s/T_{melt} = 0.5$), the discrepancy between the structural parameters of silicon and aluminum [32] in a ratio of 4 : 3 is 0.13%. This leads to the formation of islands with an average size of 130 nm, compared to 70 nm for temperatures above 400°C ($T_s/T_{melt} = 0.7$). Such large islands lose their epitaxial connection with the substrate due to the large number of structural defects (presumably misfit dislocations) that appear when the sample is cooled to room temperature. At $T_s/T_{melt} \geq 0.7$, the epitaxial connection of the (111) and (001) islands with the substrate is preserved with partial stress relaxation, primarily for the Al(001) islands.

FUNDING

This study was carried out as part of a state assignment of Valiev Institute of Physics and Technology, Russian Academy of Sciences, Russian Ministry of Education and Science on topic no. FFNN-2022-0019. The development and study of the samples was carried out at the Institute of Radio-Engineering and Electronics, Russian Academy of Sciences under a grant of the Russian Science Foundation, RSF no. 23-79 00022, https://rscf.ru/project/23-79-00022/.

CONFLICT OF INTEREST

The authors of this work declare that they have no conflicts of interest.

REFERENCES

1. Alferov, Zh.I., Binary heterostructures: Concept and applications in physics, electronics and technology, *Usp. Fiz. Nauk*, 2002, vol. 172, no. 9, p. 1068. https://doi.org/10.3367/ufnr.0172.200209e.1068
2. Saini, S., Ashok, P., and Verma, A., Dynamic multicolor switching using ultrathin vanadium oxide on aluminum-based asymmetric Fabry–Pérot resonant structure, *Appl. Phys. Lett.*, 2024, vol. 124, no. 1, p. 11105. https://doi.org/10.1063/5.0175803
3. Hass, G., Francombe, M.H., and Vossen, J.L., *Physics of Thin Films*, Advances in Research and Development, vol. 7, New York: Academic, 1982.
4. Sunil, B.S., Bellanger, P., Roques, S., Slaoui, A., Ulyashin, A.G., Leuvrey, C., and Bjorge, A.R., Formation of microcrystalline silicon layer for thin films silicon solar cells on aluminium substrates, *2016 Int. Renewable and Sustainable Energy Conf. (IRSEC)*, Marrakech, Morocco, 2016, IEEE, 2016, pp. 214–219. https://doi.org/10.1109/irsec.2016.7983910
5. Liao, W.-S. and Lee, S.-C., Interfacial interaction between Al–1% Si and phosphorus-doped hydrogenated amorphous Si alloy at low temperature, *J. Appl. Phys.*, 1997, vol. 81, no. 12, pp. 7793–7797. https://doi.org/10.1063/1.365389
6. Barajas-Valdes, U. and Suárez, O.M., Morphological and structural characterization of magnetron-sputtered

aluminum and aluminum–boron thin films, *Crystals*, 2021, vol. 11, no. 5, p. 492. https://doi.org/10.3390/cryst11050492

7. Greibe, T., Stenberg, M., Wilson, C., Bauch, T., Shumeiko, V., and Delsing, P., Are "pinholes" the cause of excess current in superconducting tunnel junctions? A study of Andreev current in highly resistive junctions, *Phys. Rev. Lett.*, 2011, vol. 106, no. 9, p. 097001. https://doi.org/10.1103/PhysRevLett.106.097001
8. Tarasov, M.A., Kuzmin, L.S., and Kaurova, N.S., Thin multilayer aluminum structures for superconducting devices, *Instrum. Exp. Tech.*, 2009, vol. 52, no. 6, pp. 877–881. https://doi.org/10.1134/s0020441209060220
9. Olausson, L., Olausson, P., and Lind, E., Gate-controlled near-surface Josephson junctions, *Appl. Phys. Lett.*, 2024, vol. 124, no. 4, p. 42601. https://doi.org/10.1063/5.0182485
10. Merkulova, I.E., Influence of synthesis parameters and thermal annealing on grain size of polycrystalline aluminum thin film, *J. Phys.: Conf. Ser.*, 2021, vol. 2119, no. 1, p. 012121. https://doi.org/10.1088/1742-6596/2119/1/012121
11. Booth, S.E., Marsh, C.D., Mallik, K., Baranauskas, V., Sykes, J.M., and Wilshaw, P.R., Fabrication of nanocrystalline aluminium islands using double-surface anodization, *J. Vac. Sci. Technol. B: Microelectron. Nanometer Struct. Process., Meas., Phenom.*, 2003, vol. 21, no. 1, pp. 316–318. https://doi.org/10.1116/1.1532025
12. Khramtsova, E.A., Zotov, A.V., Saranin, A.A., Ryzhkov, S.V., Chub, A.B., and Lifshits, V.G., Growth of extra-thin ordered aluminum films on Si(111) surface, *Appl. Surf. Sci.*, 1994, vols. 82–83, pp. 576–582. https://doi.org/10.1016/0169-4332(94)90278-x
13. Grupp, C. and Taleb-Ibrahimi, A., Hydrogen passivation at the Al/H:Si(111)-(1×1) interface, *J. Vac. Sci. Technol. A: Vac., Surf., Films*, 1998, vol. 16, no. 4, pp. 2683–2686. https://doi.org/10.1116/1.581400
14. Markov, I.V., *Crystal Growth for Beginners: Fundamentals of Nucleation, Crystal Growth and Epitaxy*, London: World Scientific, 2003.
15. Eisenmenger-Sittner, C., Growth control and thickness measurement of thin films, *Encyclopedia of Applied Physics*, Wiley, 2019, pp. 1–44. https://doi.org/10.1002/3527600434.eap809
16. Lomov, A.A., Zakharov, D.M., Tarasov, M.A., Chekushkin, A.M., Tatarintsev, A.A., Kiselev, D.A., Ilyina, T.S., and Seleznev, A.E., Influence of the homobuffer layer on the morphology, microstructure, and hardness of Al/Si(111) films, *Tech. Phys.*, 2023, vol. 68, no. 7, p. 833. https://doi.org/10.61011/TP.2023.07.56624.83-23
17. Poate, J.M., Tu, K.N., and Mayer, J.W., *Thin Films: Interdiffusion and Reactions*, New York: Wiley, 1978.
18. Reed-Hill, R.E., *Physical Metallurgy Principles*, New York: Van Nostrand, 1981, 2nd ed.
19. Fortuin, A.W., Alkemade, P.F.A., Verbruggen, A.H., Steinfort, A.J., Zandbergen, H., and Radelaar, S., Characterization of single-crystalline Al films grown on Si(111), *Surf. Sci.*, 1996, vol. 366, no. 2, pp. 285–294. https://doi.org/10.1016/0039-6028(96)00824-2
20. Barmak, K. and Coffey, K., *Metallic Films for Electronic, Optical and Magnetic Applications*, Cambridge: Woodhead Publishing, 2013.
21. Leikin, A.E. and Rodin, B.I., *Materialovedenie* (Materials Science), Moscow: Vysshaya Shkola, 1971.
22. Movchan, B.A. and Demchishin, A.V., Growth and structure of thine solid films, *Phys. Met. Metallogr.*, 1969, vol. 28, pp. 83–91.
23. Ohring, M., *Materials Science of Thin Films: Deposition and Structure*, Hoboken, N.J.: Academic, 2002.
24. Anders, A., A structure zone diagram including plasma-based deposition and ion etching, *Thin Solid Films*, 2010, vol. 518, no. 15, pp. 4087–4090. https://doi.org/10.1016/j.tsf.2009.10.145
25. Thornton, J.A., High rate thick film growth, *Annu. Rev. Mater. Sci.*, 1977, vol. 7, no. 1, pp. 239–260. https://doi.org/10.1146/annurev.ms.07.080177.001323
26. Kaiser, N., Review of the fundamentals of thin-film growth, *Appl. Opt.*, 2002, vol. 41, no. 16, p. 3053. https://doi.org/10.1364/ao.41.003053
27. D'Anterroches, C., High resolution TEM study of Al–Si 1%/Si interface, *Microscopy of Semiconducting Materials 1983: Third Oxford Conf. on Microscopy of Semiconducting Materials*, Cullis, A.G., Ed., Boca Raton, FL Fla.: CRC Press, 1983, p. 95. https://doi.org/10.1201/9781003069614
28. Hasan, M.-A., Radnoczi, G., and Sundgren, J.-E., Epitaxial growth of Al on Si (100) and Si (111) by evaporation in uhv, *Vacuum*, 1990, vol. 41, nos. 4–6, pp. 1121–1123. https://doi.org/10.1016/0042-207x(90)93886-n
29. Tjong, S.C. and Chen, H., Nanocrystalline materials and coatings, *Mater. Sci. Eng.: R: Rep.*, 2004, vol. 45, nos. 1–2, pp. 1–88. https://doi.org/10.1016/j.mser.2004.07.001
30. Wen, H.J., Dähne-Prietsch, M., Bauer, A., Cuberes, M.T., Manke, I., and Kaindl, G., Thermal annealing of the epitaxial Al/Si(111)7×7 interface: Al clustering, interfacial reaction, and Al-induced $p+$ doping, *J. Vac. Sci. Technol. A: Vac., Surf., Films*, 1995, vol. 13, no. 5, pp. 2399–2406. https://doi.org/10.1116/1.579480
31. Sosnowski, M., Ramac, S., Brown, W.L., and Kim, Yo.O., Importance of steps in heteroepitaxy: The case of aluminum on silicon, *Appl. Phys. Lett.*, 1994, vol. 65, no. 23, pp. 2943–2945. https://doi.org/10.1063/1.112541
32. Nakashima, P.N.H., The crystallography of aluminum and its alloys, *Encyclopedia of Aluminum and Its Alloys*, Totten, G.E., Tiryakioğlu, M., and Kessler, O., Eds., Boca Raton, Fla.: CRC Press, 2018, pp. 488–586. https://doi.org/10.1201/9781351045636-140000245
33. Horio, Y., Different growth modes of Al on Si(111)7 × 7 and Si(111)$\sqrt{3}$ × $\sqrt{3}$–Al Surfaces, *Jpn. J. Appl. Phys.*, 1999, vol. 38, no. 8r, p. 4881. https://doi.org/10.1143/JJAP.38.4881